Bicriteria Optimization in Multihop Wireless Networks: Characterizing the Throughput-Energy Envelope

Canming Jiang, *Member*, *IEEE*, Yi Shi, *Member*, *IEEE*, Sastry Kompella, *Senior Member*, *IEEE*, Y. Thomas Hou, *Senior Member*, *IEEE*, and Scott F. Midkiff, *Senior Member*, *IEEE*

Abstract—Network throughput and energy consumption are two important performance metrics for a multihop wireless network. Current state-of-the-art research is limited to either maximizing throughput under some energy constraint or minimizing energy consumption while satisfying some throughput requirement. Although many of these prior efforts were able to offer some optimal solutions, there is still a critical need to have a systematic study on how to optimize both objectives simultaneously. In this paper, we take a multicriteria optimization approach to offer a systematic study on the relationship between the two performance objectives. To focus on throughput and energy performance, we simplify link layer scheduling by employing orthogonal channels among the links. We show that the solution to the multicriteria optimization problem characterizes the envelope of the entire throughput-energy region, i.e., the so-called optimal throughput-energy curve. We prove some important properties of the optimal throughput-energy curve. For case study, we consider both linear and nonlinear throughput functions. For the linear case, we characterize the optimal throughput-energy curve precisely through parametric analysis, while for the nonlinear case, we use a piecewise linear approximation to approximate the optimal throughput-energy curve with arbitrary accuracy. Our results offer important insights on exploiting the tradeoff between the two performance metrics.

Index Terms—Bicriteria optimization, multihop wireless networks, throughput, energy

1 Introduction

Since the inception of multihop wireless networks, throughput and energy are two key performance metrics that network designers and operators bear in their minds. Throughput is clearly the first and foremost performance consideration, as users of a multihop wireless network increasingly wish such network can offer comparable experience as its counterpart wireline networks. On the other hand, energy consumption is also regarded as a key performance consideration, as many types of multihop wireless networks (e.g., ad hoc network, sensor network) are battery powered and are constrained with limited energy at each node.

To date, there is a vast amount of literature on optimizing throughput or energy. For network throughput, people have been trying to maximize it either at different layers (e.g., scheduling algorithms [8], [26], [36], [39], routing algorithms [6], [13], [32]) or jointly across multiple layers (e.g., [1], [2], [7], [12], [24], [27]). For energy, people are trying to conserve/minimize its consumption while meeting certain service requirements (e.g., energy-efficient scheduling and MAC schemes [17], [21], [34], [35], [38], [40], or energy-efficient routing protocol [15], [18], [23]).

We have also witnessed quite a few studies exploring the interaction between network throughput and energy consumption in the context of either maximizing network throughput under energy (or power) constraints (e.g., [9], [14], [31]) or minimizing energy consumption while satisfying some throughput constraints (e.g., [5], [10], [24], [25], [31]). The only one previous work that studied the relationship between throughput and energy is [37], which considered a particular type of cell partitioned network. Although many of these prior efforts were able to offer some optimal solutions, there is still a critical need to have a systematic study on how to optimize both objectives simultaneously. In particular, none of the existing efforts is able to offer a holistic view on how the maximum network throughput changes as a function of network energy consumption for general multihop wireless networks, i.e., the so-called optimal throughput-energy curve (or envelope) in this paper.

The significance of optimal throughput-energy curve is threefold. First, it gives an envelope of the entire throughput-energy region, which offers a global perspective on the achievable throughput-energy tradeoff. In

- *C. Jiang is with the Bradley Department of Electrical and Computer Engineering, Virginia Polytechnic Institute and State University, Blacksburg, VA 24061, and Cisco Systems Inc., 3600 Cisco Way, San Jose, CA 95134. E-mail: jcm@vt.edu.*
- *Y. Shi is with the Bradley Department of Electrical and Computer Engineering, Virginia Polytechnic Institute and State University, Blacksburg, VA 24061, and Intelligent Automation Inc., 18909 Lark Song Ter, Germantown, MD 20874. E-mail: yshi@vt.edu.*
- *S. Kompella is with the Information Technology Division, US Naval Research Laboratory, Washington, DC 20375. E-mail: sastry.kompella@nrl.navy.mil.*
- *Y.T. Hou and S.F. Midkiff are with the Bradley Department of Electrical and Computer Engineering, Virginia Polytechnic Institute and State University, 302 Whittemore Hall (0111), Blacksburg, VA 24061. E-mail: {thou, midkiff}@vt.edu.*

Manuscript received 20 May 2011; revised 14 Apr. 2012; accepted 5 July 2012; published online 17 July 2012.
For information on obtaining reprints of this article, please send e-mail to: tmc@computer.org, and reference IEEECS Log Number TMC-2011-05-0270. Digital Object Identifier no. 10.1109/TMC.2012.162.

contrast, a solution to traditional problems such as maximizing throughput under energy constraints or minimizing energy under throughput constraints only represents a point on this curve or inside this region. Second, each time when the requirement on either network throughput or energy consumption changes, one can use the optimal throughput-energy curve to find a new optimal tradeoff between throughput and energy instantly, rather than resorting to solving a new optimization problem. Finally, the optimal throughput-energy curve shows us the existence of a *saturation point*, beyond which the throughput can no longer be further increased, regardless of how much additional energy is used.

In this paper, we conduct a systematic study on the optimal relationship between network throughput and energy consumption for a multihop wireless network. We tackle this problem through a multicriteria optimization formulation, i.e., maximizing network throughput *while* minimizing total power in the network. Our main contributions can be summarized as follows:

- By solving the multicriteria optimization problem, we find the entire throughput-energy curve.
- We find a number of important properties associated with the optimal throughput-energy curve, such as nondecreasing, concave, the existence of a saturation point, and strictly increasing between zero and the saturation point.
- For the case study, we consider two cases where the throughput functions are linear and nonlinear, respectively:
  - For the linear case, we show that the optimal throughput-energy curve can be characterized exactly via parametric analysis (PA).
  - For the nonlinear case, we show that the optimal throughput-energy curve can be approximated by piecewise linear segments with arbitrary desired accuracy.

The remainder of this paper is organized as follows: In Section 2, we describe our network model. In Section 3, we present a multicriteria formulation that maximizes network throughput while minimizing energy consumption in a multihop wireless network. We show that finding the optimal solution to this multicriteria optimization problem is equivalent to finding the optimal throughput-energy curve. We also present some important properties associated with the optimal throughput-energy curve. In Section 4, we discuss approaches to obtain throughput-energy curves in practice. Sections 5 and 6 present two case studies when the throughput functions are linear and nonlinear, respectively. Section 7 concludes this paper.

2 Network Model

We consider a general multihop wireless network with a set of $\mathcal{N}$ nodes. A directed link $(i,j), i,j \in \mathcal{N}$ from nodes i to j exists if and only if node j is within the transmission range of node i. Denote $\mathcal{L}$ the set of directed links in the network. To focus on throughput and energy performance, we simplify link layer scheduling by employing orthogonal channels among the links,[1] similar to that in [12], [22], [29]. Table 1 lists all notations used in this paper.

TABLE 1
Notation

Symbol	Definition
B_l	Bandwidth on link l
C_l	Average rate of link l
d_l	Distance between the transmitter and the receiver of link l
$\mathrm{dst}(m)$	Destination node of session $m \in \mathcal{M}$
$f(P)$	The optimal throughput-energy curve
g_l	Channel gain on link l
$h(\cdot)$	A utility function
$\mathcal{L}$	The set of links in the network
$\mathcal{L}_i^{\mathrm{In}}$	The set of incoming links at node i
$\mathcal{L}_i^{\mathrm{Out}}$	The set of outgoing links at node i
$\mathcal{M}$	The set of user sessions in the network
$\mathcal{N}$	The set of nodes in the network
P	Rate of energy consumption in the network, $P = \sum_{l\in\mathcal{L}} \alpha_l \cdot (P_T + P_R)$
P_T	Rate of energy consumption for transmission at a node
P_R	Rate of energy consumption for reception at a node
$r(m)$	Data rate of session $m \in \mathcal{M}$
$r_l(m)$	Data rate on link l that is attributed to session m
$\mathrm{src}(m)$	Source node of session m
U	$= \sum_{m\in\mathcal{M}} h[r(m)]$, the network throughput utility
$w(m)$	A weight associated with session $m \in \mathcal{M}$
$\mathbf{x}$	$= \{r(m), r_l(m), \alpha_l \mid l \in \mathcal{L}, m \in \mathcal{M}\}$, a solution to our optimization problems
α_l	The fraction of time within a time frame when link l is active
γ	Path loss index
η	Ambient Gaussian noise density

Denote $\mathcal{M}$ as a set of user (unicast) communication sessions in the network. Denote $\mathrm{src}(m)$ and $\mathrm{dst}(m)$ as the source and destination nodes of session $m \in \mathcal{M}$, respectively. Denote $r(m)$ as the rate of session $m \in \mathcal{M}$. Consider a general flow routing strategy where flow splitting (i.e., multipath) is allowed. On link l, denote $r_l(m)$ as the data rate that is attributed to session $m \in \mathcal{M}$. Denote $\mathcal{L}_i^{\mathrm{Out}}$ and $\mathcal{L}_i^{\mathrm{In}}$ as the sets of potential outgoing and incoming links at node i, respectively. Then, we have the following flow balance equations for multihop routing:

- If node i is the source node of session m, i.e., $i = \mathrm{src}(m)$, then

$$\sum_{l\in\mathcal{L}_i^{\mathrm{Out}}} r_l(m) = r(m). \tag{1}$$

- If node i is an intermediate relay node along the path of session m, i.e., $i \neq \mathrm{src}(m)$ and $i \neq \mathrm{dst}(m)$, then

$$\sum_{l\in\mathcal{L}_i^{\mathrm{Out}}}^{l\neq(i,\mathrm{src}(m))} r_l(m) = \sum_{l\in\mathcal{L}_i^{\mathrm{In}}}^{l\neq(\mathrm{dst}(m),i)} r_l(m). \tag{2}$$

- If node i is the destination node of session m, i.e., $i = \mathrm{dst}(m)$, then

1. An upper bound on the number of required orthogonal channels is $1 + d_v$, where d_v is the maximum vertex degree in the conflict graph in the final flow routing solution. More efficient channel assignment algorithms may further reduce the number of required channels. But problem of channel assignment is beyond the scope of this paper.

$$\sum_{l \in \mathcal{L}_i^{\text{In}}} r_l(m) = r(m). \quad (3)$$

It can be easily verified that once (1) and (2) are satisfied, then (3) is also satisfied. As a result, it is sufficient to list only (1) and (2) in a formulation.

For power control at each node, we employ a simple "on/off" control, which has been used for energy saving in wireless networks (see, e.g., [28], [30]). When a link is "on," the transmitter of this link transmits at a fixed power level P_T; when the link is "off" (for energy conservation), the transmitter of this link does not expend any power for transmission. To quantify the percentage of time that the link is in different states, we denote α_l $(0 \le \alpha_l \le 1, l \in \mathcal{L})$ the fraction of time within a time frame that link l is "on."

Based on this on/off energy conservation model, the average rate of link l can be computed as

$$C_l = \alpha_l \cdot B_l \log_2\left(1 + \frac{P_T \cdot g_l}{\eta B_l}\right), \quad (4)$$

where B_l is the bandwidth of link l under a given channel assignment, g_l is channel gain between the transmitter and receiver of link l, and η is the ambient Gaussian noise density. Note the absence of an interference term in (4), which is due to our use of orthogonal channels in the network.

On link l, we have the following flow rate constraint:

$$\sum_{m \in \mathcal{M}} r_l(m) \le C_l, \text{ for all } l \in \mathcal{L}, \quad (5)$$

which states that the aggregate flow rates from all sessions traversing link l cannot exceed the achievable rate of this link.

3 Throughput-Energy Curve and Its Properties

3.1 Multicriteria Formulation

In this paper, we are interested in a multicriteria optimization problem, i.e., how to maximize network throughput while minimizing energy consumption at the same time. We now give a formulation of this problem.

Denote $h(\cdot)$ as a continuous, concave, and nondecreasing utility function. We define the network throughput utility U as follows:

$$U = \sum_{m \in \mathcal{M}} h[r(m)],$$

where $r(m)$ is the rate of session $m \in \mathcal{M}$. Note that in the special case when $h[r(m)] = r(m)$, then U is simply the sum of throughput in the network; in the case when $h[r(m)] = \ln[r(m)]$, U is called proportional fairness [20].

Now, we consider energy consumption. Note that when a link is active, the rate of energy consumption includes energy consumption for both transmission and reception. Then, the network energy consumption rate P in the network can be defined as follows:

$$P = \sum_{l \in \mathcal{L}} \alpha_l \cdot (P_T + P_R),$$

where α_l is the fraction of time within a time frame that link l is active, P_T is the transmission power, and P_R is the reception power. For simplicity, we assume that all nodes have the same transmission power and reception power.

With the above two definitions, our multicriteria optimization problem can be formulated as follows:

$$\begin{aligned} \text{MOPT min } & P = \sum_{l \in \mathcal{L}} \alpha_l \cdot (P_T + P_R) \\ \max\ & U = \sum_{m \in \mathcal{M}} h[r(m)] \\ \text{s.t. } & \text{Constraints (1), (2), (4), and (5)} \\ & r(m), r_l(m) \ge 0,\ 0 \le \alpha_l \le 1. \end{aligned}$$

Note that the two objective functions, P and U, are *conflicting* objectives. For example, when P is minimized (i.e., 0), U is also 0 and is not maximized. So, there does not appear to exist an optimal solution to our problem that optimizes both objectives simultaneously.

Given that an optimal solution does not exist, a natural question to ask is what kind of solutions should we pursue when investigating problem MOPT? Before answering this question, it is important to clarify how we compare two feasible solutions. We use

$$\mathbf{x} = \{r(m), r_l(m), \alpha_l \mid l \in \mathcal{L}, m \in \mathcal{M}\}$$

to represent a solution. Denote (P_1, U_1) and (P_2, U_2) the objective pairs of two different feasible solutions $\mathbf{x}_1$ and $\mathbf{x}_2$, respectively. We say objective pair (P_1, U_1) dominates (P_2, U_2) if $P_1 \le P_2$ and $U_1 \ge U_2$. This means that solution $\mathbf{x}_1$ uses no more energy than solution $\mathbf{x}_2$ to achieve the same or more throughput, i.e., $\mathbf{x}_1$ is better than $\mathbf{x}_2$. With this clarification, it is clear that our goal should be to find solutions that are not dominated by any other solutions. That is, we want to find solutions with their objective pair $(P^\dagger, U^\dagger)$ such that there does *not* exist another solution with objective pair (P, U) such that $P \le P^\dagger$ and $U \ge U^\dagger$. Such solutions are called *Pareto-optimal solutions* (also called efficient solutions in [16]) and the objective value pair $(P^\dagger, U^\dagger)$ corresponding to a Pareto-optimal solution is called a *Pareto-optimal point*. Pareto-optimal solutions are those that any further improvement in one objective will lead to a deterioration in the other objective.

For our problem, we find that it is difficult to obtain all Pareto-optimal solutions directly. Instead, we can find a solution $\mathbf{x}^*$ with its objective pair (P^*, U^*) such that there does not exist another solution $\mathbf{x}$ with its objective pair (P, U) satisfying $P < P^*$ and $U > U^*$. That is, there does not exist a solution $\mathbf{x}$ that can use less energy than solution $\mathbf{x}^*$ to achieve more throughput. Such solutions are called *weakly Pareto optimal solutions* (also called weakly efficient solutions in [16]), and the objective value pair (P^*, U^*) corresponding to such a solution is called a *weakly Pareto optimal point*. Note that Pareto-optimal points are also weakly Pareto optimal, but weakly Pareto optimal points are not always Pareto optimal. Weakly Pareto optimal solutions are those for which improvement in both objectives simultaneously is impossible, but improvement on one objective without deteriorating the other is possible. Once we find all the weakly Pareto optimal solutions, we can identify a subset of solutions that are Pareto optimal based on its definition.

3.2 Throughput-Energy Curve

Instead of solving MOPT directly, let us consider a simpler single objective optimization problem for a given P (i.e., fixing one of the objective values). That is,

$$\begin{aligned} \text{OPT}(P) \quad \max \quad & \sum_{m\in\mathcal{M}} h[r(m)] \\ \text{s.t.} \quad & \sum_{l\in\mathcal{L}} \alpha_l (P_T + P_R) = P \\ & \text{All constraints in MOPT} \\ & r(m), r_l(m) \geq 0, 0 \leq \alpha_l \leq 1. \end{aligned} \tag{6}$$

We now show that the optimal solution to $\text{OPT}(P)$ is a weakly Pareto optimal solution to MOPT.

Lemma 1. *If $\mathbf{x}^* = \{r^*(m), r_l^*(m), \alpha_l^* \mid l \in \mathcal{L}, m \in \mathcal{M}\}$ is an optimal solution to $OPT(P)$ for a given value of P^* with a corresponding objective value U^*, then $\mathbf{x}^*$ is a weakly Pareto optimal solution to MOPT.*

Lemma 1 can be proved by contradiction. The details are given in [19].

Denote the range of P as $[0, P_{max}]$, where P_{max} can be obtained by setting $\alpha_l = 1$ for all $l \in \mathcal{L}$. That is, $P_{max} = \sum_{l\in\mathcal{L}}(P_T + P_R) = |\mathcal{L}| \cdot (P_T + P_R)$. If one can enumerate all possible $P \in [0, P_{max}]$ and obtain their corresponding optimal solutions via $\text{OPT}(P)$, then based on Lemma 1, all these solutions are weakly Pareto optimal solutions.

Now, we show the converse is also true, i.e., any weakly Pareto optimal point (P, U) of MOPT can be obtained by a corresponding problem of $\text{OPT}(P)$.

Lemma 2. *Each weakly Pareto optimal point (P, U) of MOPT can be obtained by solving an instance of $OPT(P)$.*

A proof of Lemma 2 is based on contradiction. We refer readers to [19].

Based on Lemmas 1 and 2, we conclude that each weakly Pareto optimal point (P, U) of MOPT uniquely corresponds to the same (P, U) generated by an optimal solution of $\text{OPT}(P)$. Thus, by finding the optimal U for each $\text{OPT}(P)$, $P \in [0, P_{max}]$, we can obtain all the weakly Pareto optimal points of MOPT. This gives us a mapping from P to U, which we denote as $f : P \to U$. Intuitively, this says that for any weakly Pareto optimal point (P, U), $U = f(P)$ is the maximum throughput utility that the network can deliver. Note that function $U = f(P)$ defines the envelope of the entire throughput-energy region, which we formally define as follows:

Definition 1 (Optimal throughput-energy curve). *For all $P \in [0, P_{max}]$, the mapping $f : P \to U$ via solving OPT(P) constitutes an optimal throughput-energy curve $U = f(P)$.*

3.3 Key Properties

In this section, we present several interesting properties for the optimal throughput-energy curve. These properties are important for us to understand the fundamental behavior of this curve and to characterize this curve under specific throughput utility functions in the next section.

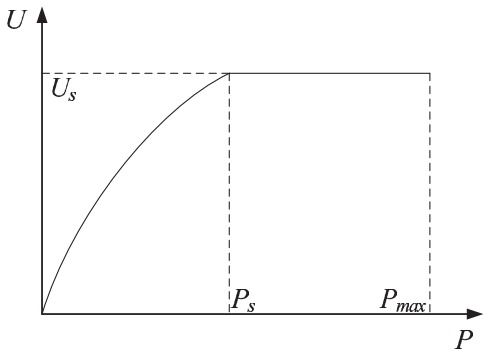

Fig. 1. The shape of an optimal throughput-energy curve.

Property 1. *$U = f(P)$ is a nondecreasing function over $0 \leq P \leq P_{max}$.*

This property is easy to understand intuitively. It says that the throughput will not decrease when energy is increased. The proof is quite straightforward and is omitted.

Property 2. *$U = f(P)$ is a concave function.*

Property 2 can be proved by the definition of a concave function. We refer readers to [19].

The next two properties further spell out the shape of the concave throughput-energy curve.

Property 3. *There is a saturation point (P_s, U_s) on the optimal throughput-energy curve $f(P)$ such that $f(P) = U_s$ for $P \in [P_s, P_{max}]$ and $f(P) < U_s$ for $P < P_s$.*

Proof. We prove this property by construction. We compute the saturation point (P_s, U_s) as follows:

We first compute the maximum achievable network throughput U_s under $\text{OPT}(P_{max})$. Once we have U_s, we can find the minimum network energy consumption rate P_s that can achieve this U_s by solving the following optimization problem:

$$\begin{aligned} P_s = \min \quad & \sum_{l\in\mathcal{L}} \alpha_l \cdot (P_T + P_R) \\ \text{s.t.} \quad & \sum_{m\in\mathcal{M}} h[r(m)] \geq U_s \\ & \text{Constraints (1), (2), (4), and (5).} \end{aligned}$$

Since a throughput-energy curve is a nondecreasing function (Property 1) and that we have $f(P_s) = f(P_{max}) = U_s$, the throughput-energy curve must be flat between $[P_s, P_{max}]$. Since P_s is the minimum energy that achieves U_s, based on Property 1, we have $f(P) < U_s$ for $P < P_s$. □

The above property states that the last segment of the optimal throughput-energy curve is *flat* after the saturation point (see Fig. 1)

The following property states that the segment of the optimal throughput-energy curve is strictly increasing for $P \in [0, P_s]$ (see Fig. 1).

Property 4. *$f(P)$ is a strictly increasing function for $P \in [0, P_s]$.*

Property 4 can be proved by contradiction. We refer readers to [19].

Recall that all the weakly Pareto optimal points of MOPT coincide with the optimal throughput-energy curve $f(P)$ over $P \in [0, P_{max}]$. It is easy to see that the points on $f(P)$ over $P \in [0, P_s]$ are Pareto-optimal points (while those on $f(P)$ over $P \in (P_s, P_{max}]$ are only weakly Pareto optimal points).

4 A Naive Approach versus Performance Guarantee

Although we have successfully analyzed some key properties of the optimal throughput-energy curve, it remains difficult to characterize the entire curve for a given throughput utility function. A naive approach to approximate the curve could be as follows: We can discretize the energy interval $[0, P_s]$ into a large number of equally spaced intervals. For each energy consumption value, P_i, we can compute its corresponding throughput value $f(P_i)$ by solving $\mathrm{OPT}(P_i)$. So, we obtain a point $(P_i, f(P_i))$ on the throughput-energy curve. Upon finding all these points on the curve, we can connect them via linear segments. This will give an approximate throughput-energy curve.

Although the above naive approach is simple and straightforward, it does not offer any performance guarantee of the curve. In contrast, one of the goals of this paper is to characterize the curve with performance guarantee. In the following two sections, we consider two classes of throughput utility functions: the linear case and the nonlinear case. In the linear case, we are able to characterize the optimal curve exactly by exploiting some special structures of linear program (LP); for the nonlinear case, we develop a novel technique to approximate the curve with $(1-\varepsilon)$-optimal performance guarantee, where ε is an arbitrary small error reflecting our desired accuracy.

5 Case 1: Linear Throughput Function

In this section, we consider the case where the throughput utility function is linear with respect to $r(m)$, $m \in \mathcal{M}$. That is, $U = \sum_{m\in\mathcal{M}} w(m)r(m)$, where $w(m)$ is a constant and can be considered as the weight for session $m \in \mathcal{M}$. In this case, our $\mathrm{OPT}(P)$ becomes the following LP:

$$\begin{aligned} \mathrm{LP}(P)\ \ \max\ & U = \sum_{m\in\mathcal{M}} w(m)r(m) \\ \text{s.t.}\ & \text{All constraints in OPT(P)} \\ & r(m), r_l(m) \geq 0,\ 0 \leq \alpha_l \leq 1. \end{aligned}$$

Instead of obtaining the $f(P)$ curve by solving $\mathrm{LP}(P)$ for all possible $P \in [0, P_{max}]$, which is impractical, we will exploit the special structure of LP and obtain the exact $f(P)$ curve by solving a *finite* number of LPs. In particular, since $\mathrm{LP}(P)$ is parametric LP with respect to P, we propose to employ the so-called PA technique [3, Ch. 6] to obtain $f(P)$ curve efficiently.

5.1 Finding $f(P)$ Curve via PA

Rewrite $\mathrm{LP}(P)$ in the standard form $\mathbf{Max\ cx}$, s.t. $\mathbf{Ax} = \mathbf{b}$ and $\mathbf{x} \geq \mathbf{0}$, where $\mathbf{A}$ is a $n_{\mathrm{row}} \times n_{\mathrm{col}}$ matrix and $\mathbf{b}$ is a n_{row} vector. Here, we use boldface to denote vectors and matrices. Assume that we have $n_{\mathrm{row}} \leq n_{\mathrm{col}}$. (Otherwise, there are more constraints than variables and will be no feasible solution in $\mathrm{LP}(P)$). Suppose that $rank(\mathbf{A}) = n_{\mathrm{row}}$.[2] A nonsingular $n_{\mathrm{row}} \times n_{\mathrm{row}}$ submatrix $\mathbf{B}$ of $\mathbf{A}$ is called basis matrix. Denote $\mathcal{B}$ as the set of indices of the columns of $\mathbf{A}$ defining $\mathbf{B}$. Set $\mathcal{B}$ is called a basis. Denote $\mathcal{Q}$ as the set of nonbasic column indices, which can be written as $\mathcal{Q} = \{1, \ldots, n_{\mathrm{col}}\} \backslash \mathcal{B}$. A solution $\mathbf{x} = \left[\begin{smallmatrix}\mathbf{x}_\mathcal{B} \\ \mathbf{x}_\mathcal{Q}\end{smallmatrix}\right]$ to equations $\mathbf{Ax} = \mathbf{b}$, where $\mathbf{x}_\mathcal{B} = \mathbf{B}^{-1}\mathbf{b}$ and $\mathbf{x}_\mathcal{Q} = 0$, is called a basic feasible solution (BFS) of the LP. The components of $\mathbf{x}_\mathcal{B}$ are called basic variables, and the components of $\mathbf{x}_\mathcal{Q}$ are called nonbasic variables. Note that the BFS of $\mathrm{LP}(P)$ is usually not unique. When a BFS $\mathbf{x} = \left[\begin{smallmatrix}\mathbf{x}_\mathcal{B} \\ \mathbf{x}_\mathcal{Q}\end{smallmatrix}\right]$ achieves the optimality of $\mathrm{LP}(P)$, we call $\mathcal{B}$ the optimal basis, and its corresponding $\mathbf{B}$ and $\mathbf{Q}$ the optimal basic matrix and the optimal nonbasic matrix.

The main idea of PA is to investigate how a perturbation on parameter P will affect the optimality of $\mathrm{LP}(P)$. For a given value of P, the current optimal basis of $\mathrm{LP}(P)$ could still be optimal when there is a perturbation on P. Thus, the interval $[0, P_s]$ can be partitioned into small consecutive intervals, each corresponding to a different optimal basis. Within each small interval, the optimal basis to $\mathrm{LP}(P)$ is the same even when P varies. Further, we will show that $f(P)$ is linear within each small interval.

Partition $[0, P_s]$ into smaller intervals. We now show how to partition interval $[0, P_s]$ into small intervals. For $\mathrm{LP}(P)$ with a particular value P, we assume that an optimal solution to $\mathrm{LP}(P)$ is $\left[\begin{smallmatrix}\mathbf{x}_\mathcal{B} \\ \mathbf{x}_\mathcal{Q}\end{smallmatrix}\right]$, and the optimal basic matrix and nonbasic matrix are $\mathbf{B}$ and $\mathbf{Q}$. Denote $\mathbf{c}_\mathcal{B}$ and $\mathbf{c}_\mathcal{Q}$ as the objective function coefficient vectors of throughput utility U for the basic and nonbasic variables, respectively. Then, we can write the corresponding canonical equations as follows [3, Ch. 6]:

$$U + \left(\mathbf{c}_\mathcal{B}^T\mathbf{B}^{-1}\mathbf{Q} - \mathbf{c}_\mathcal{Q}\right)\mathbf{x}_\mathcal{Q} = \mathbf{c}_\mathcal{B}^\mathbf{T}\mathbf{B}^{-1}\mathbf{b}, \tag{7}$$

$$\mathbf{x}_\mathcal{B} + \mathbf{B}^{-1}\mathbf{Q}\mathbf{x}_\mathcal{Q} = \mathbf{B}^{-1}\mathbf{b}. \tag{8}$$

Note that when $\mathbf{x}_\mathcal{B}$ and $\mathbf{x}_\mathcal{Q}$ are optimal solutions, we have $\mathbf{x}_\mathcal{Q} = \mathbf{0}$ [3, Ch. 3]. Thus, based on (8), we have

$$\mathbf{x}_\mathcal{B} = \mathbf{B}^{-1}\mathbf{b}\ .$$

Suppose that we do a perturbation on parameter P, i.e., we change P to $P + \delta$. Then, vector $\mathbf{b}$ becomes $\mathbf{b} + (\delta, 0, \ldots, 0)^T$. The only change due to this perturbation is that $\mathbf{B}^{-1}\mathbf{b}$ will be replaced by $\mathbf{B}^{-1}(\mathbf{b} + \delta\mathbf{I})$, where vector $\mathbf{I}$ has a single 1 on the first element and zero on all the others. Note that $\mathbf{x}_\mathcal{B} = \mathbf{B}^{-1}(\mathbf{b} + \delta\mathbf{I})$ is a BFS. As long as $\mathbf{B}^{-1}(\mathbf{b} + \delta\mathbf{I})$ is nonnegative, the current basis remains optimal. This is because that changing $\mathbf{b}$ to $\mathbf{b} + \delta\mathbf{I}$ does not affect the correctness of (7) and (8).

On the other hand, when one of the elements in $\mathbf{B}^{-1}(\mathbf{b} + \delta\mathbf{I})$ becomes negative, the optimal basis must change. Otherwise, we will have one negative element in $\mathbf{x}_\mathcal{B}$, which contradicts $\mathbf{x} \geq \mathbf{0}$ in the LP formulation. The

2. Otherwise, there are some redundant constraints, and the linear programming problem can be simplified to the case where $rank(\mathbf{A}) = n_{\mathrm{row}}$ by removing those redundant constraints.

Basis Updating Algorithm

1. **Input:** An optimal basis $\mathcal{B}$ for a given P.
2. Compute $\bar{\mathbf{A}} = \mathbf{B}^{-1}\mathbf{A}$, $\bar{\mathbf{b}} = \mathbf{B}^{-1}\mathbf{b}$, and $\bar{\mathbf{b}}' = \mathbf{B}^{-1}\mathbf{I}$.
3. If $\mathcal{S} = \{i : \bar{b}'_i < 0\} = \emptyset$, stop.
4. $\hat{\delta} = \min_{i\in\mathcal{S}} \left\{ \frac{\bar{b}_i}{-\bar{b}'_i} \right\}$.
5. $r = \arg\min_i \left\{ \frac{\bar{b}_i}{-\bar{b}'_i} \right\}$.
6. $s = \arg\min_j \left\{ \frac{\bar{b}_j}{\bar{\mathbf{A}}_{jr}}, \bar{\mathbf{A}}_{jr} < 0 \right\}$.
7. Let $\mathcal{B} = (\mathcal{B}\backslash\{r\}) \cup \{s\}$ and $\mathbf{b} = \mathbf{b} + \hat{\delta}\mathbf{I}$.
8. Update $\mathbf{B}$ based on $\mathcal{B}$ ($\mathbf{B}$ consists of $\mathbf{A}$'s columns whose indices are in $\mathcal{B}$).
9. Compute $P = P + \hat{\delta}$, $\mathbf{x} = \mathbf{B}^{-1}\mathbf{b}$ and $U = \mathbf{c}_{\mathcal{B}}^T\mathbf{x}$.
10. **Output:** The new basis $\mathcal{B}$, $\mathbf{x}$, $\hat{\delta}$ and (P, U) pair.

Fig. 2. The basis updating algorithm.

value of δ at which this change occurs can be determined as follows: Denote $\bar{\mathbf{b}} = \mathbf{B}^{-1}\mathbf{b}$ and $\bar{\mathbf{b}}' = \mathbf{B}^{-1}\mathbf{I}$, and let $\mathcal{S} = \{i : \bar{b}'_i < 0\}$, where $\bar{b}'_i$ is the ith element in vector $\bar{\mathbf{b}}'$. If $\mathcal{S} = \emptyset$, then the current basis is optimal for all values of $\delta \geq 0$ since all elements in vector $\mathbf{B}^{-1}(\mathbf{b} + \delta\mathbf{I})$ are nonnegative. Otherwise, let

$$\hat{\delta} = \min_{i\in\mathcal{S}} \left\{ \frac{\bar{b}_i}{-\bar{b}'_i} \right\}. \tag{9}$$

For $\delta \in [0, \hat{\delta}]$, the current basis $\mathbf{B}$ remains optimal, and its corresponding BFS is $\mathbf{x}_{\mathcal{B}} = \mathbf{B}^{-1}(\mathbf{b} + \delta\mathbf{I})$. When $\delta > \delta'$, the basis $\mathbf{B}$ is no longer optimal. Thus, we need to choose the variable x_r to leave the basis, where the minimum in (9) is attained for $i = r$. The entering variable x_s is chosen by the dual simplex method rule [3, Ch. 6]. Based on the new optimal basis obtained after the pivot, we can update the corresponding canonical equations and get a (P, U) pair, which is an endpoint of the linear segment of $f(P)$.

Fig. 2 lists the steps to obtain a new optimal basis for a given optimal basis $\mathcal{B}$. Thus, starting from $P = 0$, we can use this algorithm iteratively to find different bases until we reach P_s. The series of $\hat{\delta}$ for these bases will partition $[0, P_s]$ into small intervals.

The complexity of the basis updating algorithm can be analyzed as follows: The dominant computational complexity occurs in step 2: $\bar{\mathbf{A}} = \mathbf{B}^{-1}\mathbf{A}$. Note that our linear programming LP(P) has $n_{\text{row}} = (1 + 2 \mid \mathcal{L} \mid + \mid \mathcal{N} \mid - \mid \mathcal{M} \mid)$ constraints and $n_{\text{col}} = (|\mathcal{L}| \cdot |\mathcal{M}| + 2 \mid \mathcal{L} \mid + \mid \mathcal{M} \mid)$ variables. Since $\bar{\mathbf{A}} = \mathbf{B}^{-1}\mathbf{A}$ involves matrix multiplication of a $n_{\text{row}} \times n_{\text{row}}$ matrix and a $n_{\text{row}} \times n_{\text{col}}$ matrix, its complexity is $O(n_{\text{row}}^2 n_{\text{col}}) = O(|\mathcal{L}|^3|\mathcal{M}| + |\mathcal{N}|^2|\mathcal{L}||\mathcal{M}| + |\mathcal{N}||\mathcal{L}|^2|\mathcal{M}|)$.

Linearity of each small interval. For each small interval with an optimal basis, we now show that $f(P)$ is linear. Suppose interval $[0, P_s]$ is divided into K small intervals $[P_i, P_{i+1}], i = 1, \ldots, K$, where $P_1 = 0, P_{K+1} = P_s$, and the optimal basis for small $[P_i, P_{i+1}]$ is $\mathbf{B}_i$. Then, for an optimal basis $\mathbf{B}_i$ within a particular small interval $[P_i, P_{i+1}]$, the objective value of throughput $f(P), P_i \leq P \leq P_{i+1}$ can be computed as follows:

$$f(P) = \mathbf{c}_{\mathcal{B}_i}^T \mathbf{B}_i^{-1}(\mathbf{b} + \delta\mathbf{I}), \tag{10}$$

where $\delta = P - P_i$. Substituting $\delta = P - P_i$ into (10), we have

$$f(P) = \mathbf{c}_{\mathcal{B}_i}^T \mathbf{B}_i^{-1}[\mathbf{b} + (P - P_i)\mathbf{I}]. \tag{11}$$

In (11), since $\mathbf{c}_{\mathcal{B}_i}^T, \mathbf{B}_i^{-1}$, $\mathbf{b}$, $\mathbf{I}$, and P_i are constants, and P is the only variable, we conclude that $f(P)$ is a linear function of P for $P_i \leq P \leq P_{i+1}$, $i = 1, \ldots, K$. We formally state this result in the following lemma:

Lemma 3. *For the linear case, the optimal throughput-energy curve $f(P)$ is piecewise linear within $[0, P_s]$.*

Recall that by executing the basis updating algorithm sequentially, we also obtain a series of (P, U) pair and the solution $\mathbf{x}$ generating (P, U), each corresponding to an optimal basis. Since $f(P)$ is a piecewise linear line with each linear segment determined by an optimal basis, the series of (P, U) pairs are the endpoints of these linear segments. Then, by connecting these endpoints consecutively, we are able to characterize the entire optimal throughput-energy curve $f(P)$.

5.2 From Curve to a Point

By obtaining the entire optimal throughput-energy curve $f(P)$, we also have the endpoints of each line segment on $f(P)$ and the solutions of all endpoints. We now show that the solution for any point on the optimal throughput-energy curve $f(P)$ can be easily calculated through linear combination of the solutions for the endpoints (instead of solving a new LP(P)).

Assume that we want to find the solution $\mathbf{x}$ for a point (P, U) on the optimal throughput-energy curve, which lies in the line segment with two ends (P_1, U_1) and (P_2, U_2), and the optimal solutions for (P_1, U_1) and (P_2, U_2) are $\mathbf{x}_1 = \{r^{(1)}(m), r_l^{(1)}(m), \alpha_l^{(1)} \mid l \in \mathcal{L},\ m \in \mathcal{M}\}$ and $\mathbf{x}_2 = \{r^{(2)}(m), r_l^{(2)}(m), \alpha_l^{(2)} \mid l \in \mathcal{L}, m \in \mathcal{M}\}$, respectively. Then, there exists a constant $0 \leq \lambda \leq 1$ such that $P = \lambda P_1 + (1 - \lambda)P_2$. The corresponding solution $\mathbf{x} = \{r(m), r_l(m), \alpha_l \mid l \in \mathcal{L}, m \in \mathcal{M}\}$ for point (P, U) can now be computed as $\mathbf{x} = \lambda\mathbf{x}_1 + (1 - \lambda)\mathbf{x}_2$, which means that the optimal session rates $r(m)$, data flow rates $r_l(m)$ on each link l, and the fraction of active time on each link α_l in solution $\mathbf{x}$ are just a simple linear combination of solutions $\mathbf{x}_1$ and $\mathbf{x}_2$.

Thus, after we characterize the optimal throughput-energy curve $f(P)$, we can find an optimal solution for any point on the curve via linear combination of known solutions. We formally state this result in the following theorem:

Theorem 1. *Denote $\mathbf{x}_i$ and $\mathbf{x}_{i+1}$ as the optimal solutions for the two endpoints $(P_i, f(P_i))$ and $(P_{i+1}, f(P_{i+1}))$ of the ith linear segment in $f(P)$. The optimal solution $\mathbf{x}$ for any point $(P, f(P))$ between $(P_i, f(P_i))$ and $(P_{i+1}, f(P_{i+1}))$, where $P = \lambda P_i + (1 - \lambda)P_{i+1}, 0 \leq \lambda \leq 1$, can be written as $\mathbf{x} = \lambda\mathbf{x}_i + (1 - \lambda)\mathbf{x}_{i+1}$.*

Proof. Based on Lemmas 1 and 2, we know that $(P, f(P))$ can be obtained by solving LP(P). Now, we need to show that the optimal solution of LP(P), where $P = \lambda P_i + (1 - \lambda)P_{i+1}, 0 \leq \lambda \leq 1$, is $\lambda\mathbf{x}_i + (1 - \lambda)\mathbf{x}_{i+1}$. From the previous analysis, we know that basis $\mathbf{B}_i$ remains optimal for LP(P), $P \in [P_i, P_{i+1}]$. Rewrite LP(P), LP(P_i), and LP(P_{i+1}) under standard forms as **Max** $\mathbf{cx}$, s.t. $\mathbf{Ax} = \mathbf{b}$ and $\mathbf{x} \geq \mathbf{0}$, **Max** $\mathbf{cx}$, s.t. $\mathbf{Ax} = \mathbf{b}_i$ and $\mathbf{x} \geq \mathbf{0}$, and **Max** $\mathbf{cx}$, s.t. $\mathbf{Ax} = \mathbf{b}_{i+1}$ and $\mathbf{x} \geq \mathbf{0}$, respectively. The

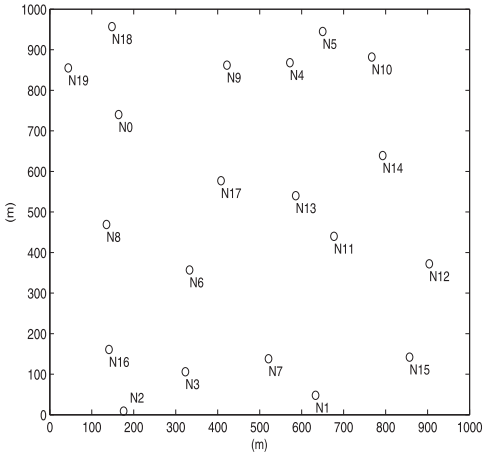

Fig. 3. Topology for a 20-node network.

TABLE 2
Source and Destination Nodes of Each Session

Session m	Source Node	Destination Node
1	N19	N15
2	N8	N12
3	N9	N3
4	N3	N5
5	N5	N1
6	N1	N12
7	N4	N11
8	N6	N10
9	N16	N6
10	N2	N10

only difference among $\mathbf{b}$, $\mathbf{b}_i$, and $\mathbf{b}_{i+1}$ is on the first element. The first elements of $\mathbf{b}$, $\mathbf{b}_i$, and $\mathbf{b}_{i+1}$ are P, P_i, and P_{i+1}. Since $P = \lambda P_i + (1-\lambda)P_{i+1}$, we have

$$\mathbf{b} = \lambda \mathbf{b}_i + (1-\lambda)\mathbf{b}_{i+1}. \tag{12}$$

We also know that the optimal solutions of LP(P), LP(P_i), and LP(P_{i+1}) are $\mathbf{x} = \mathbf{B}_i^{-1}\mathbf{b}$, $\mathbf{x}_i = \mathbf{B}_i^{-1}\mathbf{b}_i$, and $\mathbf{x}_{i+1} = \mathbf{B}_i^{-1}\mathbf{b}_{i+1}$. Based on (12), we can conclude $\mathbf{x} = \lambda \mathbf{x}_i + (1-\lambda)\mathbf{x}_{i+1}$. This completes the proof. □

5.3 A Numerical Example

In the following, we present some pertinent numerical results to demonstrate our theoretical findings. We first describe our simulation settings. As shown in Fig. 3, we consider a randomly generated multihop wireless network with 20 nodes, which are distributed in a square region of $1{,}000\ \text{m} \times 1{,}000\ \text{m}$. The transmission power and reception power for each node are set to $P_T = 1$ W and $P_R = 0.2$ W. The bandwidth on each link is $B_l = 1$ MHz. We use a simplified channel gain model $g_l = d_l^{-\gamma}$, where d_l is the distance between the transmitter and receiver of link l, and γ is the path loss index. We set $\gamma = 3$. There are 10 user sessions in the network, and Table 2 specifies the source and destination nodes of each session. For the weight $w(m)$ of each session $m \in \mathcal{M}$, we consider two scenarios: 1) equal weight, for example, $w(m) = 1$ for all $m \in \mathcal{M}$; and 2) random weight for each session.

The top curve in Fig. 4a shows the throughput-energy curve when each session has an equal weight of 1. At the saturation point, we have $P_s = 50.12$ W and $U_s = 120.02$. This curve is obtained by using the PA method, which gives

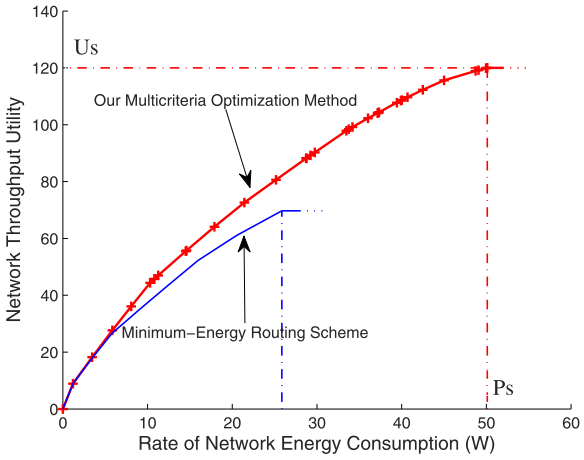

(a) Equal weight

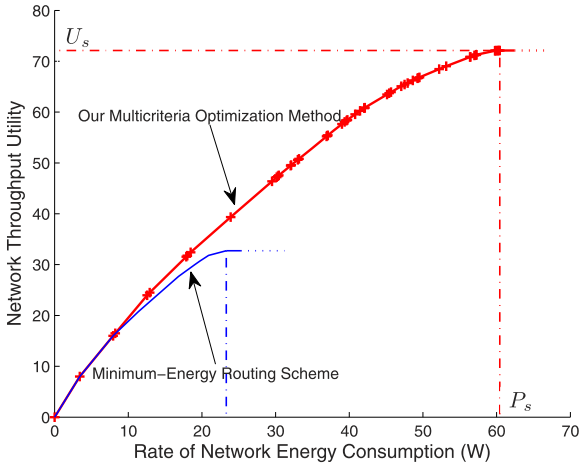

(b) Unequal weight

Fig. 4. The throughput-energy curves for a 20-node example.

33 endpoints that interconnect the piecewise linear segments of $f(P)$. For comparison, the bottom curve in Fig. 4a shows the throughput-energy curve under the popular minimum energy routing scheme [33], where each session chooses the path that consumes the minimum energy. The minimum energy path for a session can be computed by using the well-known shortest path algorithms (e.g., Dijkstra's algorithm [11]), where the cost on link l is set to the total energy consumed to send one bit from a transmitter to a receiver, i.e., $(P_T + P_R)/C_l$. The large gap between throughput utility of the two curves shows that minimum-energy routing is far from optimal in terms of throughput-energy curve. This result affirms the importance of employing multicriteria formulation as we have done in this paper.

Fig. 4b shows the results for the case when the weight of each session is randomly chosen. The randomly generated weights for the 10 sessions are 0.8147, 0.1270, 0.9134, 0.9134, 0.6324, 0.0975, 0.2785, 0.5469, 0.1270, and 0.9058, respectively. Again, the throughput-energy curve is of the same form as that in Fig. 4a, as expected. At the saturation point, we have $P_s = 60.43$ W and $U_s = 72.11$. The bottom curve in Fig. 4b shows the throughput-energy curve under minimum energy routing, which is far from optimal.

TABLE 3
α_l for Each Active Link l in the Example for the Saturation Point

Active link	α_l	Active link	α_l	Active link	α_l	Active link	α_l	Active link	α_l
$(0,8)$	1.00	$(4,10)$	1.00	$(8,16)$	0.92	$(12,15)$	0.11	$(16,6)$	1.00
$(0,9)$	1.00	$(4,14)$	1.00	$(8,17)$	1.00	$(13,11)$	1.00	$(16,8)$	1.00
$(0,17)$	1.00	$(5,10)$	1.00	$(9,0)$	1.00	$(13,14)$	1.00	$(17,6)$	0.84
$(0,18)$	0.02	$(6,3)$	1.00	$(9,4)$	0.69	$(14,10)$	1.00	$(17,9)$	0.97
$(1,15)$	1.00	$(6,8)$	0.92	$(9,5)$	1.00	$(14,11)$	1.00	$(17,11)$	1.00
$(2,3)$	1.00	$(6,13)$	1.00	$(9,17)$	1.00	$(14,12)$	0.64	$(17,13)$	0.99
$(3,6)$	1.00	$(6,17)$	1.00	$(9,18)$	0.89	$(14,13)$	0.28	$(18,0)$	0.78
$(3,7)$	0.85	$(7,6)$	1.00	$(10,14)$	1.00	$(15,12)$	0.98	$(18,9)$	0.02
$(4,5)$	0.54	$(8,0)$	1.00	$(11,12)$	1.00	$(16,2)$	0.95	$(19,0)$	0.10
$(4,9)$	0.71	$(8,6)$	1.00	$(12,11)$	0.55	$(16,3)$	1.00		

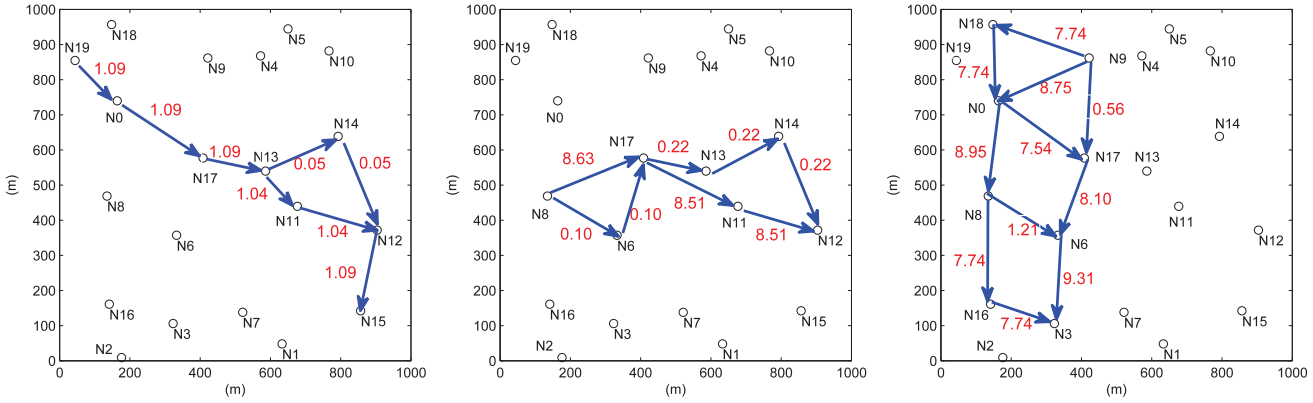

(a) Session 1 (b) Session 2 (c) Session 3

Fig. 5. The optimal flow routing solutions for Sessions 1, 2, and 3 for the saturation point (50.12, 120.02) in the example.

Note that for each endpoint on the curve, we also obtain its optimal solution for multihop routing variables $r(m)$, $r_l(m)$, and α_l at each link. As an example, we show the optimal solution for the saturation point $(P_s, U_s) = (50.12, 120.02)$ under equal weight, which uses the minimum energy consumption of 50.12 W to achieve the maximum network throughput of 120.02 Mb/s. We find that the optimal data rates (in Mb/s) for the 10 sessions are 1.09, 8.73, 17.05, 4.40, 0, 9.45, 25.90, 22.44, 30.96, and 0, respectively.[3] In this optimal solution, there are 49 active links in the network. Table 3 shows the fraction of time for each active link. Also, we find that some links never need to be activated to maximize throughput utility. Fig. 5 shows the flow routing solution for Sessions 1, 2, and 3 (others are similar and are thus omitted). The number next to each arrow represents the data rate on that link that is attributed to that session.

6 Case 2: Nonlinear Throughput Function

In this section, we consider the case where the throughput utility function $h(\cdot)$ is a concave, but nonlinear function of $r(m), m \in \mathcal{M}$. In particular, we consider $h[r(m)] = \ln[r(m)], m \in \mathcal{M}$, which is called *proportional fairness* in [20]. In this case, for a given P, OPT(P) is a convex, nonlinear program. Although convex program OPT(P) can be solved efficiently for one given P, it is impractical to solve an *infinite* number of such convex problems when P varies from 0 to P_{max}. Further, due to nonlinearity, we cannot take advantage of the PA technique to compute the *exact* optimal throughput-energy curve efficiently.

Instead of finding the exact optimal throughput-energy curve, we propose a piecewise linear approximation for this curve, where the approximation is guaranteed to be within $(1-\varepsilon)$-optimal, with ε being an arbitrary small number.

6.1 Finding $f(P)$ Curve with $(1-\varepsilon)$ Optimality

Note that for a given P, we can always find a corresponding U on the optimal throughput-energy curve by solving a convex program (see Lemma 1). So, the question becomes how to choose a set of such points and connect them with piecewise linear segments so that this piecewise linear approximation is no more than ε (in percentile) from the unknown optimal throughput-energy curve.

First, we identify the two endpoints on the optimal throughput-energy curve that we want to approximate. On the left side, since the throughput utility is a $\ln(\cdot)$ function, it is negative when P is small. Assuming that we are only interested in the optimal throughput-energy curve when $f(P) \geq 0$, we will pick a P, denoted as P_0, such that $U_0 = f(P_0)$ is just above zero.[4] On the right side, recall that the optimal throughput-energy curve $f(P)$ is flat from $P = P_s$ to $P = P_{max}$. So, we can choose the saturation point (P_s, U_s) (see Section 3 on how to obtain it) as our right endpoint.

3. We are aware that there is a fairness issue in this solution, due to the network throughput being defined as the weighted sum of all session rates. In the next session, we will show that fairness issue can be addressed when the throughput utility function is defined in terms of $\ln(\cdot)$.

4. Note that $f(P_0) = 0$ cannot be our left endpoint due to the singularity it presents when we compute the approximation error (in percentile).

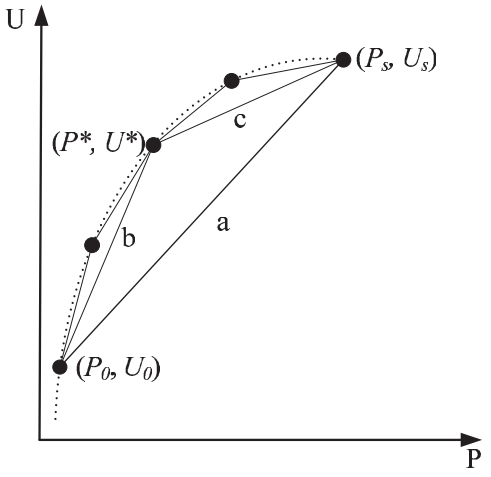

Fig. 6. An illustration of our piecewise linear approximation method.

With our two endpoints on the optimal throughput-energy curve being (P_0, U_0) and (P_s, U_s), our approximation method works as follows (see Fig. 6). We connect points (P_0, U_0) and (P_s, U_s) with a linear segment a and consider it as our first approximation of the optimal throughput-energy curve. To examine if linear segment a is accurate enough, we compute an error upper bound σ of this approximation (in percentile). This is not trivial and will be shown in Lemma 4. If $\sigma \leq \varepsilon$, then our linear approximation is considered accurate enough and we are done. Otherwise, we will find a point (P^*, U^*) on the optimal throughput-energy curve and use two linear segments b and c as a better approximation. Again, finding this point (P^*, U^*) is not trivial (since the complete optimal throughput-energy curve is unknown) and will be explained shortly. Now the same process continues on linear segments b and c. The process continues until $\sigma \leq \varepsilon$ for every linear segment of the piecewise linear approximation curve.

We first show how to compute (P^*, U^*), since we need (P^*, U^*) when computing σ.

Finding (P^*, U^*). Point (P^*, U^*) has the maximum approximation error when we use a line segment to approximate a segment of the optimal throughput-energy curve (see Fig. 7).

Suppose that (P_1, U_1) and (P_2, U_2) are two endpoints of a line segment, which we denote as $\tilde{f}(P)$. Then, this line segment $\tilde{f}(P)$ can be characterized as $\tilde{f}(P) = U_1 + \frac{U_2 - U_1}{P_2 - P_1}(P - P_1)$, $P_1 \leq P \leq P_2$. Although the optimal throughput-energy curve $f(P)$ is unknown, we imagine that we move line $\tilde{f}(P)$ upward until it is tangential to the curve. Denote this tangential point as (P^*, U^*), which is the point having the maximum absolute (rather than percentile) approximation error if we were to use $\tilde{f}(P)$ to approximate $f(P)$. Then, we have

$$\begin{aligned} & f(P^*) - \tilde{f}(P^*) \\ &= \max\{f(P) - \tilde{f}(P)\} \\ &= \max\left\{\sum_{m \in \mathcal{M}} h[r(m)] - \left[U_1 + \frac{U_2 - U_1}{P_2 - P_1}(P - P_1)\right]\right\}, \end{aligned}$$

for $P_1 \leq P \leq P_2$. Therefore, the tangential point (P^*, U^*) can be found by solving the following optimization problem:

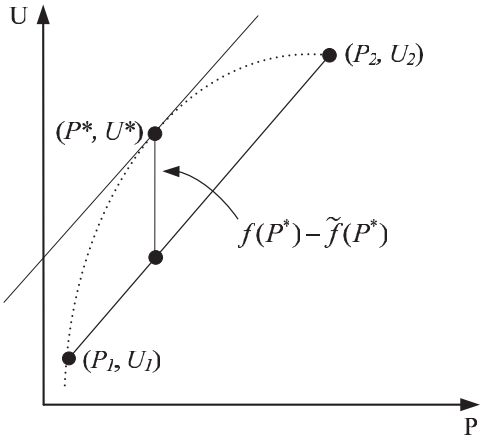

Fig. 7. An illustration showing how to obtain the tangential point and maximum approximation error on one linear segment.

$$\begin{aligned} \text{P-MAX} \quad \max \quad & \sum_{m \in \mathcal{M}} h[r(m)] - \left[U_1 + \frac{U_2 - U_1}{P_2 - P_1}(P - P_1)\right] \\ \text{s.t.} \quad & \sum_{l \in \mathcal{L}} \alpha_l (P_T + P_R) - P = 0 \\ & \text{All constraints in MOPT} \\ & P_1 \leq P \leq P_2. \end{aligned}$$

Note that in the above optimization problem, P is a variable, which is different from $\text{OPT}(P)$. The above optimization problem is a convex problem, which can be solved efficiently by using subgradient method [4, Ch. 8].

Finding σ. After obtaining the tangential point (P^*, U^*), we can calculate an upper bound σ of the approximation error (in percentile) with the following lemma:

Lemma 4. *By using $\tilde{f}(P)$ to approximate $f(P)$ for $P_1 \leq P \leq P_2$, an upper bound for this approximation error (in percentile) is*

$$\sigma = \frac{1}{1 + \frac{U_1}{U^* - \tilde{f}(P^*)}}.$$

Proof. Referring to Fig. 7, for any point $(P, f(P))$ within $[P_1, P_2]$, the approximation error (in percentile) is

$$\frac{f(P) - \tilde{f}(P)}{f(P)} = \frac{f(P) - \tilde{f}(P)}{f(P) - \tilde{f}(P) + \tilde{f}(P)} = \frac{1}{1 + \frac{\tilde{f}(P)}{f(P) - \tilde{f}(P)}}.$$

Since $\tilde{f}(P) \geq f(P_1) = U_1$ and $f(P) - \tilde{f}(P) \leq U^* - \tilde{f}(P^*)$, we have

$$\frac{f(P) - \tilde{f}(P)}{f(P)} = \frac{1}{1 + \frac{\tilde{f}(P)}{f(P) - \tilde{f}(P)}} \leq \frac{1}{1 + \frac{U_1}{U^* - \tilde{f}(P^*)}} = \sigma.$$

□

Now, given that we can compute σ at each iteration and our process stops when $\sigma \leq \varepsilon$ for each segment, it is not hard to see that our piecewise linear approximation can guarantee $(1 - \varepsilon)$-optimality. We state this result in the following theorem:

Theorem 2. *For any small $\varepsilon > 0$, the proposed piecewise linear approximation method can approximate the optimal throughput-energy curve $f(P)$ with $(1 - \varepsilon)$-optimality.*

Our proposed piecewise linear approximation method involves computing a sequence of convex programming problems. In theory, the worst-case complexity of convex programming problems is NP-hard. But in practice, most convex programming problems (including ours) can be solved efficiently. For the numerical example in Section 6.3, it only took several seconds for our method to find the approximated curve.

6.2 From Approximated Curve to a Point

We have shown how to obtain a throughput-energy curve with $(1-\varepsilon)$-optimal performance guarantee. Next, we show that for any point $(P, f(P))$ on the optimal (unknown) throughput-energy curve, we can obtain a solution (which includes session rates, data flow rates, and the fraction of time for each link) with $(1-\varepsilon)$-optimality through linear combination of the solutions that we already have for the endpoints on the approximated curve. Note that this is much faster than solving a new convex programming problem (OPT(P)). We formally state this result in the following theorem:

Theorem 3. *Denote $\mathbf{x}_i$ and $\mathbf{x}_{i+1}$ as the optimal solutions for the two endpoints $(P_i, \tilde{f}(P_i))$ and $(P_{i+1}, \tilde{f}(P_{i+1}))$ of the ith linear segment on the approximated curve $\tilde{f}(P)$. Denote $(P, f(P))$ as a point on the optimal curve, where $P = \lambda P_i + (1-\lambda)P_{i+1}$, $P_i \le P \le P_{i+1}$, $0 \le \lambda \le 1$. Then, the point $(P, \hat{U})$ generated by the solution $\hat{\mathbf{x}} = \lambda \mathbf{x}_i + (1-\lambda)\mathbf{x}_{i+1}$ is within $(1-\varepsilon)$-optimal from point $(P, f(P))$.*

Proof. We first show that $\hat{\mathbf{x}}$ is a feasible solution to MOPT. Note that solutions $\mathbf{x}_i$ and $\mathbf{x}_{i+1}$ are obtained by solving P-MAX. It is easy to see that $\mathbf{x}_i$ and $\mathbf{x}_{i+1}$ satisfy all the constraints in MOPT. Since the constraints in MOPT define a convex region, $\hat{\mathbf{x}} = \lambda \mathbf{x}_i + (1-\lambda)\mathbf{x}_{i+1}$ is also in this region. Thus, $\hat{\mathbf{x}}$ is feasible to MOPT.

For the energy consumption by solution $\hat{\mathbf{x}}$, it is easy to show that it is equal to P.

Next, we show that throughput $\hat{U}$ under $\hat{\mathbf{x}}$ is at least $\tilde{f}(P)$. That is, the throughput $\hat{U}$ under $\hat{\mathbf{x}}$ is greater than or equal to the throughput corresponding to the same P on the approximated curve.

Denote $\{r^{(i)}(m) \mid m \in \mathcal{M}\}$ and $\{r^{(i+1)}(m) \mid m \in \mathcal{M}\}$ as the session data rates in solutions $\mathbf{x}_i$ and $\mathbf{x}_{i+1}$, respectively. Then, we have that the session data rates in $\hat{\mathbf{x}}$ are $\{\lambda r^{(i)}(m) + (1-\lambda) r^{(i+1)}(m) \mid m \in \mathcal{M}\}$. Thus, we get

$$\begin{aligned}
\hat{U} &= \sum_{m\in\mathcal{M}} h[\lambda r^{(i)}(m) + (1-\lambda) r^{(i+1)}(m)] \\
&\ge \sum_{m\in\mathcal{M}} \{\lambda h[r^{(i)}(m)] + (1-\lambda) h[r^{(i+1)}(m)]\} \\
&= \lambda \tilde{f}(P_i) + (1-\lambda)\tilde{f}(P_{i+1}) \\
&= \tilde{f}[\lambda P_i + (1-\lambda) P_{i+1}] \\
&= \tilde{f}(P),
\end{aligned}$$

where the second inequality holds due to the concavity of function $h(\cdot)$ and the fourth inequality holds since $\tilde{f}(P)$ is linear for $P_i \le P \le P_{i+1}$.

Since $\hat{\mathbf{x}}$ is a feasible solution to MOPT and $(P, f(P))$ is Pareto optimal, we have $\hat{U} \le f(P)$. Since $(P, \tilde{f}(P))$ is on the approximated curve with $(1-\varepsilon)$-optimal and $\tilde{f}(P) \le \hat{U} \le f(P)$, we can conclude that $(P, \hat{U})$ is also $(1-\varepsilon)$-optimal. □

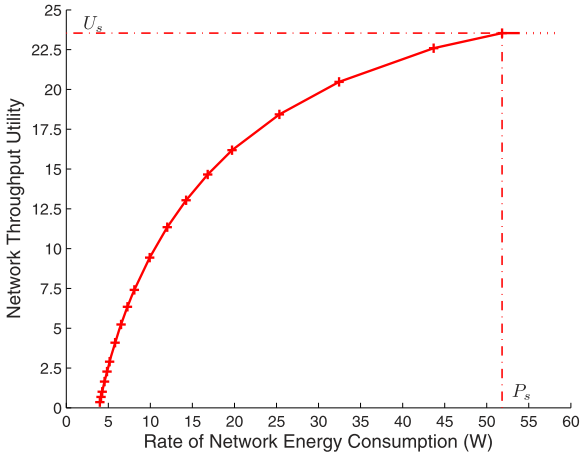

Fig. 8. A $(1-\varepsilon)$-optimal throughput-energy curve for the nonlinear case. $\varepsilon = 1\%$.

6.3 A Numerical Example

We now use a numerical example to illustrate the optimal throughput-energy curve when the throughput utility function $h[r(m)] = \ln[r(m)]$. We use the same setting as that of the numerical example shown in Section 5. The network topology is shown in Fig. 3. We first determine the saturation point (P_s, U_s) based on the approach presented in Section 3. On the left, we find $P(3.86) = 0$. So, we choose $P_0 = 4 > 3.86$ and find its corresponding throughput utility $f(P_0) = 0.35$. On the right, we find the saturation point $(P_s, U_s) = (51.83, 23.54)$. Now, we will approximate the optimal throughput-energy curve $f(P)$ for $P \in [4.00, 51.83]$. Suppose we set the target approximation error $\varepsilon = 1\%$, i.e., we are pursuing a 99 percent-optimal piecewise linear approximation. Using the method described in this section, we obtain 18 piecewise linear segments shown in Fig. 8, corresponding to linear connection of 19 points on the optimal throughput-energy curve. From the figure, we can see that these points are not equally spaced along the horizontal axis. Our method dynamically adds points on the curve to meet the error bound requirement. When the curve grows rapidly at the beginning, we put more points there; when the curve slows its growth toward the end, fewer points are needed. On the other hand, if the naive approach were employed to divide the same interval $[P_0, P_s]$ into 18 equally spaced smaller intervals, the maximum error bound among all intervals would be 48 percent.

As an example, we show the optimal solution (including session rates, data flow rates, and the fraction of time for each active link) for saturation point $(P_s, U_s) = (51.83, 23.54)$. The optimal data rates (in Mb/s) for the 10 sessions are 8.90, 9.35, 11.87, 7.84, 11.27, 8.40, 12.00, 11.78, 20.89, and 7.67, respectively. Note that unlike the linear case under equal weight, where there is a fairness issue, there is no session that has zero rate under the nonlinear case. This is due to our choice of $\ln(\cdot)$ as the throughput utility function. There are 57 active links in the network. In Table 4, we show the fraction of time for each active link. We also show the

TABLE 4
α_l for Each Active Link l in the Example for the Saturation Point under Nonlinear Case

Active link	α_l	Active link	α_l	Active link	α_l	Active link	α_l	Active link	α_l
$(0, 8)$	1.00	$(4, 14)$	1.00	$(8, 16)$	0.61	$(13, 6)$	0.65	$(16, 8)$	1.00
$(0, 9)$	1.00	$(5, 9)$	0.62	$(8, 17)$	1.00	$(13, 11)$	0.89	$(17, 6)$	0.91
$(0, 17)$	1.00	$(5, 10)$	0.75	$(9, 0)$	1.00	$(13, 14)$	1.00	$(17, 9)$	1.00
$(0, 18)$	0.02	$(6, 3)$	1.00	$(9, 4)$	0.74	$(14, 4)$	0.02	$(17, 11)$	1.00
$(1, 15)$	1.00	$(6, 7)$	1.00	$(9, 5)$	1.00	$(14, 10)$	1.00	$(17, 13)$	0.90
$(2, 3)$	0.54	$(6, 8)$	0.22	$(9, 17)$	1.00	$(14, 11)$	1.00	$(18, 0)$	0.02
$(2, 16)$	0.60	$(6, 13)$	1.00	$(9, 18)$	0.02	$(14, 12)$	1.00	$(18, 9)$	0.05
$(3, 1)$	0.43	$(6, 17)$	1.00	$(10, 14)$	0.89	$(14, 13)$	0.80	$(19, 0)$	0.78
$(3, 6)$	1.00	$(7, 1)$	0.74	$(11, 12)$	1.00	$(15, 12)$	0.98	$(19, 18)$	0.02
$(3, 7)$	0.85	$(7, 6)$	1.00	$(11, 14)$	0.75	$(16, 2)$	0.44		
$(4, 5)$	0.16	$(8, 0)$	1.00	$(12, 14)$	1.00	$(16, 3)$	1.00		
$(4, 10)$	1.00	$(8, 6)$	0.64	$(12, 15)$	0.12	$(16, 6)$	1.00		

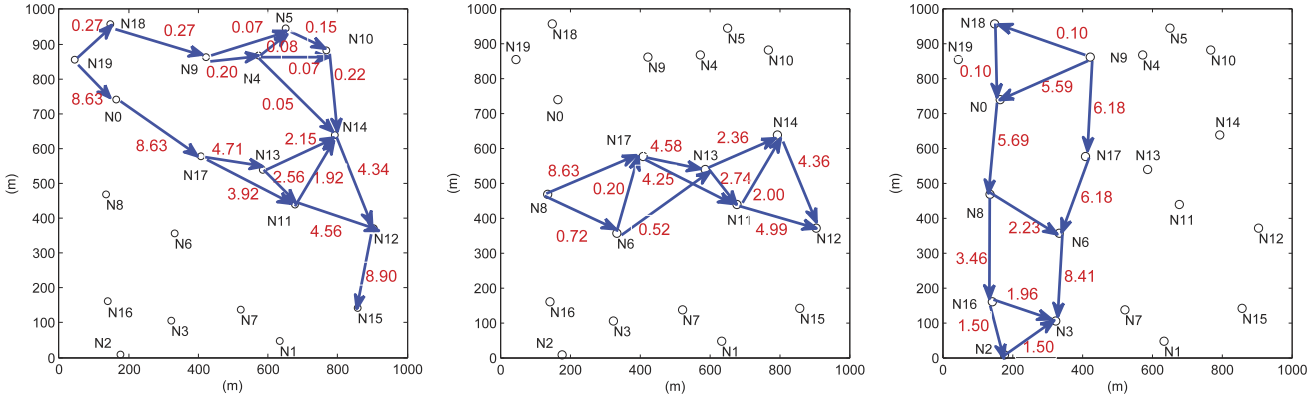

(a) Session 1 (b) Session 2 (c) Session 3

Fig. 9. The flow routing solutions for Sessions 1, 2, and 3 for the saturation point (51.83, 23.54) in the example.

optimal flow routing solutions for the first three sessions in Fig. 9, but omit to show the rest to conserve space.

7 Conclusion

In this paper, we explored the relationship between two key performance metrics for a multihop wireless network: network throughput and energy consumption. By casting the problem into a multicriteria optimization, we showed that the solution to this problem characterizes the envelope of the entire throughput-energy region. Subsequently, we presented a number of important properties associated with the optimal throughput-energy curve. As for case study, we considered both the linear and nonlinear throughput functions. For the linear case, we were able to characterize the optimal throughput-energy curve precisely via PA. For the nonlinear case, we proposed a piecewise linear approximation that can guarantee $(1 - \varepsilon)$-optimal.

In theory, the characterization of optimal throughput-energy curve is a major step beyond the state-of-the-art research, which is limited to either maximizing throughput under some energy constraint or minimizing energy consumption, while satisfying some throughput requirement (with each being able to offer only a single point on the optimal throughput-energy curve). In practice, the optimal throughput-energy curve is very useful for a network designer or operator, as it offers a holistic view on the two performance metrics. A network designer/operator can achieve his/her desired tradeoff between the two metrics depending on the specific network application scenarios.

Acknowledgments

This research was supported in part by the US National Science Foundation under grants 0925719, 1064953, and 1247830, and ONR under grant N000141310080. The work of S. Kompella was supported in part by the ONR.

References

[1] M. Al-Ayyoub and H. Gupta, "Joint Routing, Channel Assignment, and Scheduling for Throughput Maximization in General Interference Models," *IEEE Trans. Mobile Computing*, vol. 9, no. 4, pp. 553-565, Apr. 2010.

[2] M. Alicherry, R. Bhatia, and L. Li, "Joint Channel Assignment and Routing for Throughput Optimization in Multi-Radio Wireless Mesh Networks," *Proc. ACM MobiCom*, pp. 58-72, Aug. 2005.

[3] M.S. Bazaraa, J.J. Jarvis, and H.D. Sherali, *Linear Programming and Network Flows*, third ed. John Wiley & Sons, 2005.

[4] M.S. Bazaraa, H.D. Sherali, and C.M. Shetty, *Nonlinear Programming: Theory and Algorithms*, third ed. John Wiley & Sons, 2006.

[5] R. Bhatia and M. Kodialam, "On Power Efficient Communication over Multi-Hop Wireless Networks: Joint Routing, Scheduling and Power Control," *Proc. IEEE INFOCOM*, pp. 1457-1466, Mar. 2004.

[6] S. Chachulski, M. Jennings, S. Katti, and D. Katabi, "Trading Structure for Randomness in Wireless Opportunistic Routing," *Proc. ACM Special Interest Group on Data Comm. (SIGCOMM '07)*, pp. 169-180, Aug. 2007.

[7] D. Chafekar, V.S.A. Kumar, M. Marathe, S. Parthasarathy, and A. Srinivasan, "Approximation Algorithms for Computing Capacity of Wireless Networks with SINR Constraints," *Proc. IEEE INFOCOM*, pp. 1166-1174, Apr. 2008.

[8] P. Chaporkar, K. Kar, and S. Sarkar, "Throughput Guarantees through Maximal Scheduling in Wireless Networks," *Proc. 43rd Ann. Allerton Conf. Comm., Control and Computing*, pp. 1557-1567, Sept. 2005.

[9] M. Chiang, "Balancing Transport and Physical Layers in Wireless Multihop Networks: Jointly Optimal Congestion Control and Power Control," *IEEE J. Selected Areas in Comm.*, vol. 23, no. 1, pp. 1166-1174, Jan. 2005.
[10] S. Cui, A.J. Goldsmith, and A. Bahai, "Energy-Constrained Modulation Optimization," *IEEE Trans. Wireless Comm.*, vol. 4, no. 5, pp. 2349-2360, Sept. 2005.
[11] T.J. Cormen, C.E. Leiserson, R.L. Rivest, and C. Stein, *Introduction to Algorithms*, second ed. MIT, 2001.
[12] L. Chen, S.H. Low, M. Chiang, and J.C. Doyle, "Cross-Layer Congestion Control, Routing and Scheduling Design in Ad Hoc Wireless Networks," *Proc. IEEE INFOCOM*, Apr. 2006.
[13] D.S.J. De Couto, D. Aguayo, J. Bicket, and R. Morris, "A High-Throughput Path Metric for Multi-Hop Wireless Routing," *Springer Wireless Networks*, vol. 11, no. 4, pp. 419-434, July 2005.
[14] R.L. Cruz and A.V. Santhanam, "Optimal Routing, Link Scheduling, and Power Control in Multi-Hop Wireless Networks," *Proc. IEEE INFOCOM*, pp. 702-711, Mar./Apr. 2003.
[15] Q. Dong, S. Banerjee, M. Adler, and A. Misra, "Minimum Energy Reliable Paths Using Unreliable Wireless Links," *Proc. ACM MobiHoc*, pp. 449-459, May 2005.
[16] M. Ehrgott, *Multicriteria Optimization*. Springer-Verlag, 2005.
[17] A. El Gamal, C. Nair, B. Prabhakar, E. Uysal-Biyikoglu, and S. Zahedi, "Energy-Efficient Scheduling of Packet Transmissions over Wireless Networks," *Proc. IEEE INFOCOM*, pp. 1773-1782, June 2002.
[18] W.R. Heinzelman, A. Chandrakasan, and H. Balakrishnan, "Energy-Efficient Communication Protocol for Wireless Microsensor Networks," *Proc. 33rd Hawaii Int'l Conf. System Sciences*, pp. 3005-3014, Jan. 2000.
[19] C. Jiang, Y. Shi, Y.T. Hou, and S. Kompella, "On Optimal Throughput-Energy Curve for Multi-Hop Wireless Networks," technical report, Bradley Dept. of Electrical and Computer Eng., Virginia Polytechnic Inst. and State Univ., http://filebox.vt.edu/users/cmjiang/Jiang10TR.pdf, July 2010.
[20] F.P. Kelly, A. Maulloo, and D. Tan, "Rate Control in Communication Networks: Shadow Prices, Proportional Fairness and Stability," *J. Operational Research Soc.*, vol. 49, no. 3, pp. 237-252, Mar. 1998.
[21] Y. Kim, H. Shin, and H. Cha, "Y-MAC: An Energy-Efficient Multi-Channel MAC Protocol for Dense Wireless Sensor Networks," *Proc. Seventh Int'l Conf. Information Processing in Sensor Networks*, pp. 53-63, Apr. 2008.
[22] M. Kodialam and T. Nandagopal, "Characterizing Achievable Rates in Multi-Hop Wireless Mesh Networks with Orthogonal Channels," *IEEE/ACM Trans. Networking*, vol. 13, no. 4, pp. 868-880, Aug. 2005.
[23] S. Kwon and N.B. Shroff, "Unified Energy-Efficient Routing for Multi-Hop Wireless Networks," *Proc. IEEE INFOCOM*, pp. 430-438, Apr. 2008.
[24] W. Li and H. Dai, "Optimal Throughput and Energy Efficiency for Wireless Sensor Networks: Multiple Access and Multipacket Reception," *EURASIP J. Wireless Comm. and Networking*, vol. 5, no. 4, pp. 541-553, Sept. 2005.
[25] L. Lin, X. Lin, and N.B. Shroff, "Low-Complexity and Distributed Energy Minimization in Multihop Wireless Networks," *IEEE/ACM Trans. Networking*, vol. 18, no. 2, pp. 501-514, Apr. 2010.
[26] X. Lin and N.B. Shroff, "The Impact of Imperfect Scheduling on Cross-Layer Congestion Control in Wireless Networks," *IEEE/ACM Trans. Networking*, vol. 14, no. 2, pp. 302-315, Apr. 2006.
[27] X. Lin and S. Rasool, "Distributed and Provably Efficient Algorithms for Joint Channel-Assignment, Scheduling, and Routing in Multichannel Ad Hoc Wireless Networks," *IEEE/ACM Trans. Networking*, vol. 17, no. 6, pp. 1874-1887, Dec. 2009.
[28] G. Lu, N. Sadagopan, B. Krishnamachari, and A. Goel, "Delay Efficient Sleep Scheduling in Wireless Sensor Networks," *Proc. IEEE INFOCOM*, pp. 2470-2481, Mar. 2005.
[29] I. Maric and R.D. Yates, "Cooperative Multihop Broadcast for Wireless Networks," *IEEE J. Selected Areas in Comm.*, vol. 22, no. 6, pp. 1080-1088, Aug. 2004.
[30] H. Nama, M. Chiang, and N. Mandayam, "Utility-Lifetime Trade-Off in Self-Regulating Wireless Sensor Networks: A Cross-Layer Design Approach," *Proc. IEEE Int'l Conf. Comm. (ICC '06)*, pp. 3511-3516, June 2006.
[31] M.J. Neely, "Energy Optimal Control for Time Varying Wireless Networks," *IEEE Trans. Information Theory*, vol. 52, no. 7, pp. 2915-2934, July 2006.
[32] M.J. Neely and R. Urgaonkar, "Optimal Backpressure Routing in Wireless Networks with Multi-Receiver Diversity," *Elsevier Ad Hoc Networks*, vol. 7, no. 5, pp. 862-881, July 2009.
[33] S. Singh, M. Woo, and C.S. Raghavendra, "Power-Aware Routing in Mobile Ad Hoc Networks," *Proc. ACM MobiCom*, pp. 181-190, Oct. 1998.
[34] Y. Sun, S. Du, O. Gurewitz, and D.B. Johnson, "DW-MAC: A Low Latency, Energy Efficient Demand-Wakeup MAC Protocol for Wireless Sensor Networks," *Proc. ACM MobiHoc*, pp. 53-62, May 2008.
[35] A. Tarello, J. Sun, M. Zafer, and E. Modiano, "Minimum Energy Transmission Scheduling Subject to Deadline Constraints," *Springer Wireless Networks*, vol. 14, no. 5, pp. 633-645, 2008.
[36] L. Tassiulas and A. Ephremides, "Stability Properties of Constrained Queueing Systems and Scheduling Policies for Maximum Throughput in Multihop Radio Networks," *IEEE Trans. Automatic Control*, vol. 37, no. 12, pp. 1936-1948, Dec. 1992.
[37] R. Urgaonkar and M.J. Neely, "Capacity Region, Minimum Energy, and Delay for a Mobile Ad-Hoc Network," *Proc. Int'l Symp. Modeling and Optimization Mobile, Ad Hoc and Wireless Networks (WiOpt)*, p. 10, Apr. 2006.
[38] T. Van Dam and K. Langendoen, "An Adaptive Energy-Efficient MAC Protocol for Wireless Sensor Networks," *Proc. ACM First Int'l Conf. Embedded Networked Sensor Systems (SenSys '03)*, pp. 171-180, Nov. 2003.
[39] X. Wu and R. Srikant, "Regulated Maximal Matching: A Distributed Scheduling Algorithm for Multi-Hop Wireless Networks with Node-Exclusive Spectrum Sharing," *Proc. IEEE Int'l Conf. Decision and Control (CDC)*, pp. 5342-5347, Dec. 2005.
[40] W. Ye, J. Heidemann, and D. Estrin, "An Energy-Efficient MAC Protocol for Wireless Sensor Networks," *Proc. IEEE INFOCOM*, pp. 1567-1576, June 2002.

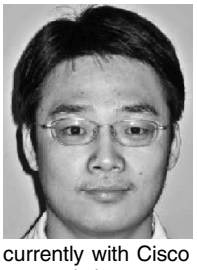

Canming Jiang received the BE degree in electrical engineering and information science from the University of Science and Technology of China, Hefei, in 2004, and the MS degree in computer science from the Graduate School, Chinese Academy of Sciences, Beijing, in 2007. During 2007-2012, he worked toward the PhD degree in the Bradley Department of Electrical and Computer Engineering at the Virginia Polytechnic Institute and State University. He is currently with Cisco Systems, Inc., in San Jose, California. His current research interests are to explore new fundamental understandings of emerging wireless networks, such as cognitive radio networks and MIMO wireless networks. He is a member of the IEEE.

Yi Shi received the PhD degree in computer engineering from the Virginia Polytechnic Institute and State University (Virginia Tech), Blacksburg, in 2007. He is currently an adjunct assistant professor in the Bradley Department of Electrical and Computer Engineering at Virginia Tech and a research scientist at Intelligent Automation Inc., Rockville, Maryland. His research focuses on algorithms and optimization for cognitive radio networks, MIMO and cooperative communication networks, sensor networks, and ad hoc networks. He received the IEEE INFOCOM 2008 Best Paper Award and the only Best Paper Award runner-up at IEEE INFOCOM 2011. He has served on technical program committees for major international conferences (including ACM MobiHoc and IEEE INFOCOM). He is a member of the IEEE.

Sastry Kompella received the PhD degree in electrical and computer engineering from the Virginia Polytechnic Institute and State University, Blacksburg, in 2006. He is currently the head of the Wireless Network Theory Section in the Information Technology Division at the US Naval Research Laboratory, Washington, DC. His research focuses on cross-layer design, optimization, and scheduling in wireless networks. He is a senior member of the IEEE.

Y. Thomas Hou received the PhD degree in electrical engineering from the Polytechnic Institute of New York University in 1998. From 1997 to 2002, he was a researcher at the Fujitsu Laboratories of America, Sunnyvale, California. Since 2002, he has been with the Bradley Department of Electrical and Computer Engineering at the Virginia Polytechnic Institute and State University, Blacksburg, where he is currently a professor. His research interests are in cross-layer optimization for wireless networks. Specifically, he is most interested in how to make significant improvement for network layer performance by exploiting new advances at the physical layer. He has published extensively in leading IEEE journals and top-tier IEEE/ACM conferences and received five Best Paper Awards from IEEE (including the IEEE INFOCOM 2008 Best Paper Award and the IEEE ICNP 2002 Best Paper Award) and one Best Paper Award from ACM. He is currently serving as an area editor of *IEEE Transactions on Wireless Communications* and as an editor for the *IEEE Transactions on Mobile Computing* and *IEEE Wireless Communications.* He was a technical program cochair of IEEE INFOCOM 2009 and is currently serving as the chair of the IEEE INFOCOM steering committee. He coedited the textbook *Cognitive Radio Communications and Networks: Principles and Practices* (Academic Press/Elsevier, 2010). He is a senior member of the IEEE.

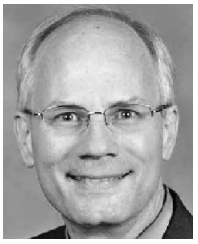

Scott F. Midkiff received the BSE and PhD degrees from Duke University, Durham, North Carolina, and the MS degree from Stanford University, California, all in electrical engineering. He joined the Virginia Polytechnic Institute and State University, Blacksburg, in 1986, where he is currently a professor in the Bradley Department of Electrical and Computer Engineering and the vice president for information technology and the chief information officer. He was previously with Bell Laboratories and held a visiting position at Carnegie Mellon University, Pittsburgh, Pennsylvania. During 2006-2009, he served as a program director at the US National Science Foundation. His research and teaching interests include wireless and ad hoc networks, network services for pervasive computing, and cyber-physical systems. He is a senior member of the IEEE.